

スイッチトポロジを有する粒子群最適化について

佐野, 亮介 / SANO, Ryosuke

(発行年 / Year)

2013-03-24

(学位授与年月日 / Date of Granted)

2013-03-24

(学位名 / Degree Name)

修士(工学)

(学位授与機関 / Degree Grantor)

法政大学 (Hosei University)

2012年度 修士論文

論文題名 スイッチトポロジーを有する
粒子群最適化について

指導教授 斎藤 利通 教授

法政大学大学院工学研究科

電気工学専攻修士課程

学生証番号： 11R3120

サノ リョウスケ

氏名 佐野 亮介

Abstract

This paper is a collection of the three papers [1][2][3] that presented by the author at international conference in the past.

The first chapter is "Basic Characteristics of Deterministic PSO with Rotational Dynamics". In this chapter, we discuss the dynamic characteristics of the Particle Swarm Optimization (PSO). We introduce the canonical deterministic particle swarm optimization (CD-PSO) where the deterministic parameters are normalized and the dynamics is described by a canonical form equation. By using the CD-PSO, we were analyzed effects of random number in the standard PSO.

The second chapter is "PSO-based Multiple Optima Search Systems with Switched Topology". In this chapter, we introduce the switched topology and solve multiple optima problems. We propose two switching rule, i.e., "random switching" that is switched by a random number, "elite preservation switching" that was depending on the value of Pbest. Further, we consider an application to analysis of the discrete dynamical systems.

The third chapter is "Particle Swarm Optimization with Switched Topology and Deterministic Parameters". In this chapter, we discuss the topology with distance. We evaluate the topology based on the average path length. Although switched topology is dynamic and the distance cannot be calculated, however we have quantified the distance using a switching probability as switching path length. We examine a relationship between switching path length and its searching performance.

目次

| | |
|--|-----------|
| 第 1 章 Basic Characteristics of Deterministic PSO with Rotational Dynamics | 7 |
| 1.1 Introduction | 7 |
| 1.2 Standard PSO | 7 |
| 1.3 Canonical Deterministic PSO | 8 |
| 1.4 Dynamics and bias of searching | 10 |
| 1.5 Numerical Experiments | 10 |
| 1.6 Conclusions | 11 |
| 第 2 章 PSO-based Multiple Optima Search Systems with Switched Topology | 13 |
| 2.1 Introduction | 13 |
| 2.2 Particle swarm optimization | 14 |
| 2.2.1 Standard PSO | 14 |
| 2.2.2 Canonical Deterministic PSO | 14 |
| 2.3 Topology of network structure | 16 |
| 2.3.1 Undirected topology | 16 |
| 2.3.2 Directed topology | 16 |
| 2.4 Switched topology | 17 |
| 2.4.1 Random switching | 18 |
| 2.4.2 Elite preservation switching | 19 |
| 2.4.3 Comparison with the stochastic PSO | 19 |
| 2.4.4 Summary of experimental results | 20 |
| 2.5 Exploring periodic points of dynamical systems | 20 |

| | | |
|--------------|---|-----------|
| 2.6 | Conclusions | 21 |
| 第 3 章 | Particle Swarm Optimization with Switched Topology and Deterministic | |
| | Parameters | 25 |
| 3.1 | Introduction | 25 |
| 3.2 | Particle swarm optimization | 26 |
| 3.2.1 | Standard PSO | 26 |
| 3.2.2 | Canonical Deterministic PSO | 26 |
| 3.3 | Topology of network structure | 27 |
| 3.3.1 | Average distance | 28 |
| 3.4 | Switched topology | 28 |
| 3.4.1 | Switching rate | 29 |
| 3.4.2 | Switching distance | 29 |
| 3.5 | Simulation | 30 |
| 3.5.1 | Search process | 30 |
| 3.5.2 | Results | 31 |
| 3.6 | Conclusions | 31 |
| | 参考文献 | 34 |
| | 研究業績 | 36 |
| | 謝辞 | 38 |

目 次

| | | |
|-----|---|----|
| 1.1 | Trajectory of three dimensional projection of ten dimensional variable space and searched space | 9 |
| 1.2 | Search process of Sphere function (f_1) | 11 |
| 1.3 | Search process of Rotated ellipsoidal function (f_2) | 12 |
| 2.1 | Network topology. Blue particles are neighbor of the red particle. | 14 |
| 2.2 | Contour map of the Himmelblau function where colder color denotes lower height. The red crosses denote the multi-solution. | 17 |
| 2.3 | Result of Himmelblau function | 18 |
| 2.4 | Switched topology | 19 |
| 2.5 | Elite preservation switching | 20 |
| 2.6 | Contour maps of the evaluation functions where colder color denotes lower height. | 22 |
| 2.7 | f_{Ikeda1} for fixed points of the Ikeda map. | 23 |
| 2.8 | f_{Ikeda2} for 2-periodic points and fixed points of the Ikeda map. | 23 |
| 2.9 | f_{Henon5} for 5-periodic points and fixed point of Henon map. | 24 |
| 3.1 | The trajectory of the CD-PSO in the phase space | 27 |
| 3.2 | Network topologies. Blue particles are neighbor of the red particle. | 28 |
| 3.3 | Switching distance | 29 |
| 3.4 | Contour maps of the benchmark functions where the red crosses denote the multi-solution. | 31 |

| | | |
|-----|---|----|
| 3.5 | Search process of $f_2(\mathbf{x})$ using the normal ring topology ($P_{\text{sw}} = 100\%$). Blue crosses denote L_{best} . Solid lines denote branch of switch-on. Dotted lines denote branch of switch-off. Red crosses denote solutions are found. | 32 |
| 3.6 | Same as Fig. 3.5 except for the switched ring topology ($P_{\text{sw}} = 25\%$). | 32 |
| 3.7 | The average distance effects the performance which is evaluated by the average number of the found optimal solutions (#SOL) for each benchmark functions. Full, Ring2, Ring, D-ring2 and D-ring are defined in Fig. 3.2. | 33 |

表 目 次

| | | |
|-----|--|----|
| 1.1 | Results | 12 |
| 2.1 | Parameter configuration for the benchmark problem | 17 |
| 2.2 | Undirected topology | 17 |
| 2.3 | Directed topology | 18 |
| 2.4 | Condition of periodic points search | 21 |
| 3.1 | The basic data of topologies in the case of 20 particles | 29 |
| 3.2 | Benchmark functions | 30 |
| 3.3 | Parameter configuration for the benchmark problems | 30 |

第1章 Basic Characteristics of Deterministic PSO with Rotational Dynamics

1.1 Introduction

Particle swarm optimization (PSO) is a meta-heuristic algorithm for solving optimization problems, proposed by J. Kennedy and R. Eberhart [4][5]. PSO is applicable to variety of problems that neural networks, power electronics and such [6][7]. The PSO generates to search velocity towards known candidate solutions. The system contains random numbers as stochastic factor, therefore it is difficult to analysis of dynamics and parameter settings. In order to analyze the dynamics of PSO, M. Clerc, and J. Kennedy proposed Deterministic PSO (D-PSO) system, that removes the stochastic factor from the standard PSO [8]. D-PSO (and PSO) is difficult to set parameters, since stability is determined by the relationship of the parameters w , c_1 and c_2 [10]. We have proposed Canonical Deterministic PSO (CD-PSO) that transformed D-PSO into canonical form [9][10][11]. Its stability determined by only one parameter Δ .

On the other hand, PSO dynamics significantly change depending on method of setting random numbers. Similarly, CD-PSO dynamics depends on method of setting the parameter of rotation angle.

This paper discusses the differences of the dynamics between the standard PSO and the CD-PSO.

1.2 Standard PSO

The standard PSO in a D-dimensional search space is described as

$$\begin{aligned} v_d^n &\leftarrow v_d^n + c_1 r_{1d}^n (Pbest_d^n - x_d^n) + c_2 r_{2d}^n (Gbest_d - x_d^n) \\ x_d^n &\leftarrow x_d^n + v_d^n \end{aligned} \quad (1.1)$$

$x_d^n \in \mathfrak{R}$ denotes the location and $v_d^n \in \mathfrak{R}$ denotes the velocity, where $n = 1 \sim N$ is index of the particle, and $d = 1 \sim D$ is index of the dimension. $Pbest_d^n \in \mathfrak{R}$ is called a personal best, it means the location of d -th dimension that gives the best value of the evaluation function of the n -th particle in the past history. $Gbest_d \in \mathfrak{R}$ is called a global best, it means the location of d -th dimension that gives the best value in the evaluation function of all particles. Standard PSO has three parameters of w , c_1 and c_2 . w is inertia weight coefficient, c_1 and c_2 are acceleration coefficients. $r_{1d}^n \in [0, 1]$ and $r_{2d}^n \in [0, 1]$ are uniform random numbers and be independent of each other. They are following two definitions.

Scalar random number (PSOs)

The random number of each dimension is the same value in the n -th particle.

Vector random number (PSOv)

The random number of each dimension is different value in the n -th particle.

We adopted the parameters that are recommended in M. Clerc and J. Kennedy's paper [8][12].

$$\begin{cases} w = 0.729 \\ c_1 = c_2 = 1.49445 \end{cases} \quad (1.2)$$

1.3 Canonical Deterministic PSO

The CD-PSO in a D-dimensional search space is described as

$$\begin{bmatrix} x_d^n \\ v_d^n \end{bmatrix} = \Delta \begin{bmatrix} \cos \theta_d^n & -\sin \theta_d^n \\ \sin \theta_d^n & \cos \theta_d^n \end{bmatrix} \begin{bmatrix} x_d^n - p_d^n \\ v_d^n \end{bmatrix} + \begin{bmatrix} p_d^n \\ 0 \end{bmatrix} \quad (1.3)$$

$$p_d^n \equiv \gamma Pbest_d^n + (1 - \gamma) Gbest_d \quad (1.4)$$

where p_d^n denotes the target location that determined from the personal best and global best. CD-PSO has three parameters of γ , Δ and θ_d^n . The parameter γ controls the mixture rate of the personal best and global best, Δ is damping factor that controls convergence of particles. θ_d^n is rotation angle that controls the frequency and sampling interval of the search. We adopt two kinds of setting for rotation angle by using basis angle ϕ .

Single rotation angle (SA)

The rotation angle of each dimension and each particle is the same value, where

$$\theta_d^n = \phi \quad (1.5)$$

Multiple rotation angle (MA)

The rotation angle of each dimension and each particle is different value, where

$$\theta_d^n = [\{ (n - 1)D + d \} \phi] \bmod 360^\circ \quad (1.6)$$

In the case of D=3 and N=10, the parameters are as follows:

$$\begin{bmatrix} \theta_1^1 & \theta_2^1 & \theta_3^1 \\ \theta_1^2 & \theta_2^2 & \theta_3^2 \\ \vdots & & \\ \theta_1^{10} & \theta_2^{10} & \theta_3^{10} \end{bmatrix} = \begin{bmatrix} \phi & 2\phi & 3\phi \\ 4\phi & 5\phi & 6\phi \\ \vdots & & \\ 28\phi & 29\phi & 30\phi \end{bmatrix}$$

Based on our trial-and-error testing, the parameters are determined as

$$\begin{cases} \gamma = 0.0 \\ \Delta = 0.95 \\ \phi = 180(3 - \sqrt{5}) = 137.51^\circ \end{cases} \quad (1.7)$$

The value adopted in ϕ is the golden angle that often appears in nature and is known as a suitable angle to fill the circle. Perhaps most prominent example is a sequence of sunflower seeds.

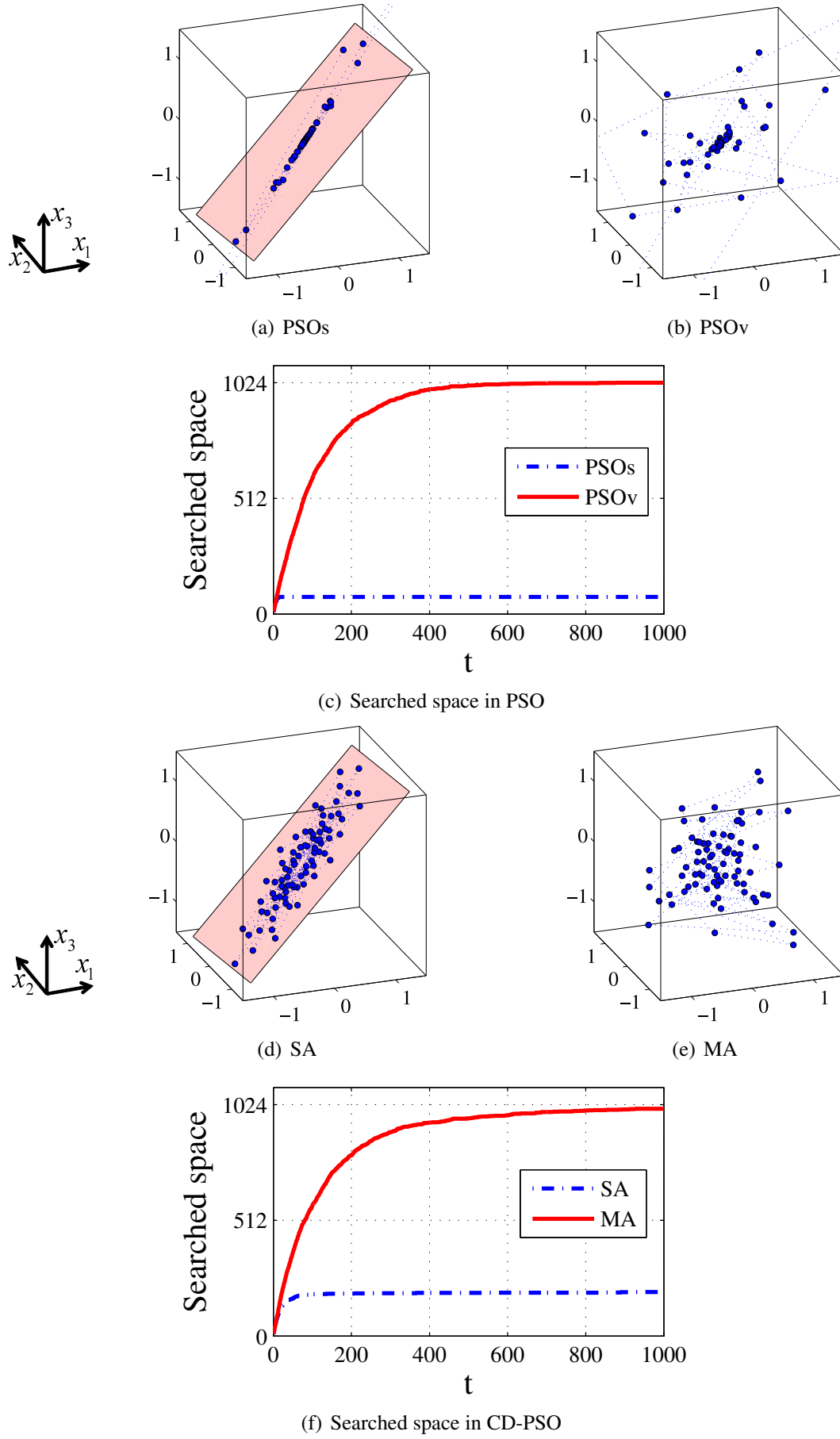


Fig 1.1: Trajectory of three dimensional projection of ten dimensional variable space and searched space

1.4 Dynamics and bias of searching

In order to compare the difference of the dynamics of the algorithms, we perform some numerical simulations under the conditions that $Gbest_d$ and $Pbest_d^n$ are fixed to the origin. Figures 1.1(a), (b), (d) and (e) show a three dimensional projection of ten dimensional variable space in PSOs, PSOV, SA, and MA, respectively. The particles of PSOs and SA are constrained on certain hyper-plane as shown in Fig. 1.1(a) and Fig. 1.1(d). It is attributed to the fixed phase difference between each dimension at location and velocity. In the PSOV and MA, because the random number and rotation angle is different each dimension, the particle is searching without bias.

In order to quantify the bias of searching, we divided the search area into half-space relative to the origin in each dimension. Furthermore we measured whether particles searched it or not. Examples of three-dimensional space, it is divided into eight half-space. Namely, each half-space is defined as $\{(+, +, +), (+, +, -), (+, -, +), \dots, (-, -, -)\}$.

Figures 1.1(c) and 1.1(f) illustrate the time fluctuation of the number of searched half-spaces. In this case, the evaluation function consists 10 dimensional variable, and the system has 10 particles. It is divided into 1024 half-spaces. In the PSOs and SA, increasing searched space is stop soon. In the PSOV and MA, the number of searched half-spaces is increased smoothly, and it converges to the maximum number. These results clearly indicate that there exists a bias in PSOs and SA searching. Furthermore demonstrate the similarity between each PSOs and SA, PSOV and MA.

1.5 Numerical Experiments

We carry out the numerical simulation using some well-known benchmark test functions to confirm the effects of the bias of searching. We adopted the unimodal function to benchmark for two reasons. First, it can surely find a good solution if searching every neighborhood. Second, it is unaffected by local solutions. The numerical simulations are carried out applying the two unimodal functions under the following conditions:

$$D = 10, N = 10, t_{max} = 1000, Trials = 1000$$

1) Sphere function (f_1)

$$f_1(\mathbf{x}) = \sum_{i=1}^D x_i^2 \quad (1.8)$$

$x_i \in [-64, 64]$, the global minimum is $\mathbf{x}^* = (0, \dots, 0)$ with $f_1(\mathbf{x}^*) = 0$. It is unimodal and separable function.

2) Rotated ellipsoidal function (f_2)

$$f_2(\mathbf{x}) = \sum_{i=1}^D \left(\sum_{k=1}^i x_k \right)^2 \quad (1.9)$$

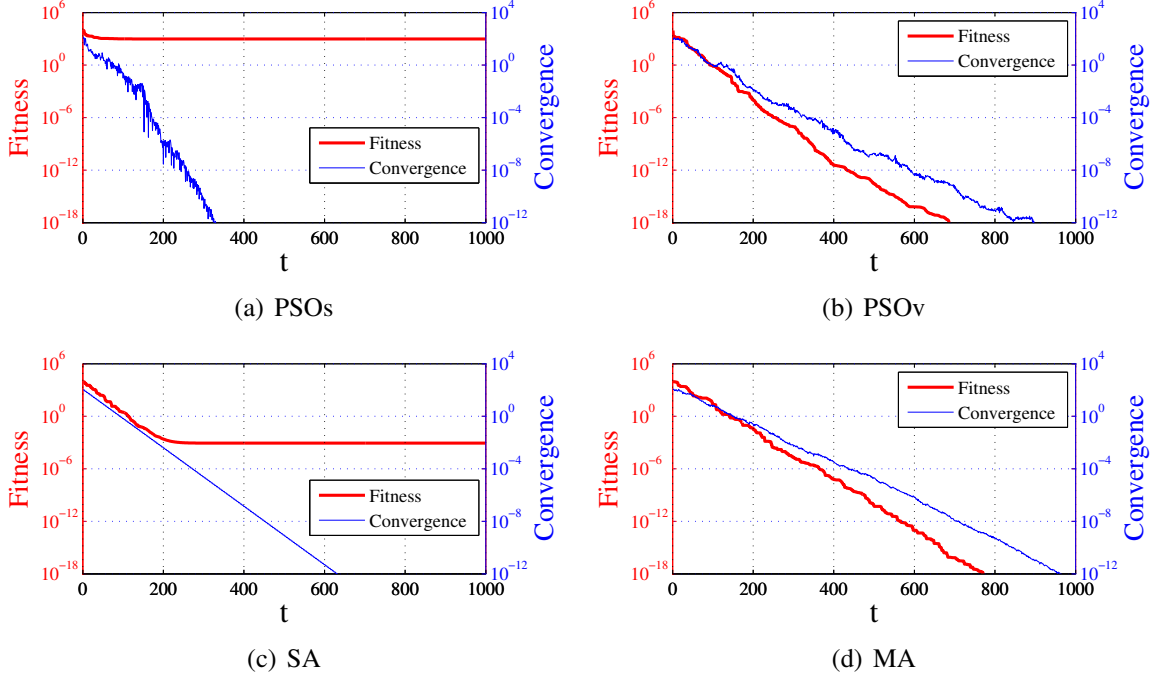
$x_i \in [-64, 64]$, the global minimum is $\mathbf{x}^* = (0, \dots, 0)$ with $f_2(\mathbf{x}^*) = 0$. It is unimodal and non-separable function.

To measure the degree of convergence of the particles, we used the following equation:

$$\text{Conv}g = \frac{1}{N} \sum_{n=1}^N \sqrt{\sum_{d=1}^D [x_d^n - \bar{x}_d]^2} \quad (1.10)$$

$$\bar{x}_d = \frac{1}{N} \sum_{n=1}^N x_d^n$$

Conv g represent the average of the Euclidean distance from the center of the particle swarm.



⊗ 1.2: Search process of Sphere function (f_1)

Figures 1.2 and 1.3 show an examples of search process on the f_1 and f_2 . In the PSO and SA, we can see that the Conv g decreases quickly, furthermore fitness stagnated soon. In contrast, in others, we can see that the Conv g decreases slowly, furthermore fitness decrease to continues. This is consistent with the results expected from described above. Comparing the two functions, f_2 is more difficult to search the optimum value than f_1 since f_2 is non-separable. The convergence time of the PSOb and MA depend on the difficulty of the benchmark function, however other cases show the similar in each function.

The results are summarized in Table 1.1. The PSOb and MA can realize better fitness than the PSOs and SA. MA shows slightly better performance than PSOb, which suggests the usefulness of CD-PSO.

1.6 Conclusions

This paper described the PSO dynamics by random number, and the CD-PSO dynamics by rotation angle. Our numerical simulation results indicated that the PSOb and MA are useful to search optimum solution than the PSOs and SA system. In summary, the searching diversity of the PSOb and MA depends on behavior of each dimension of the particle.

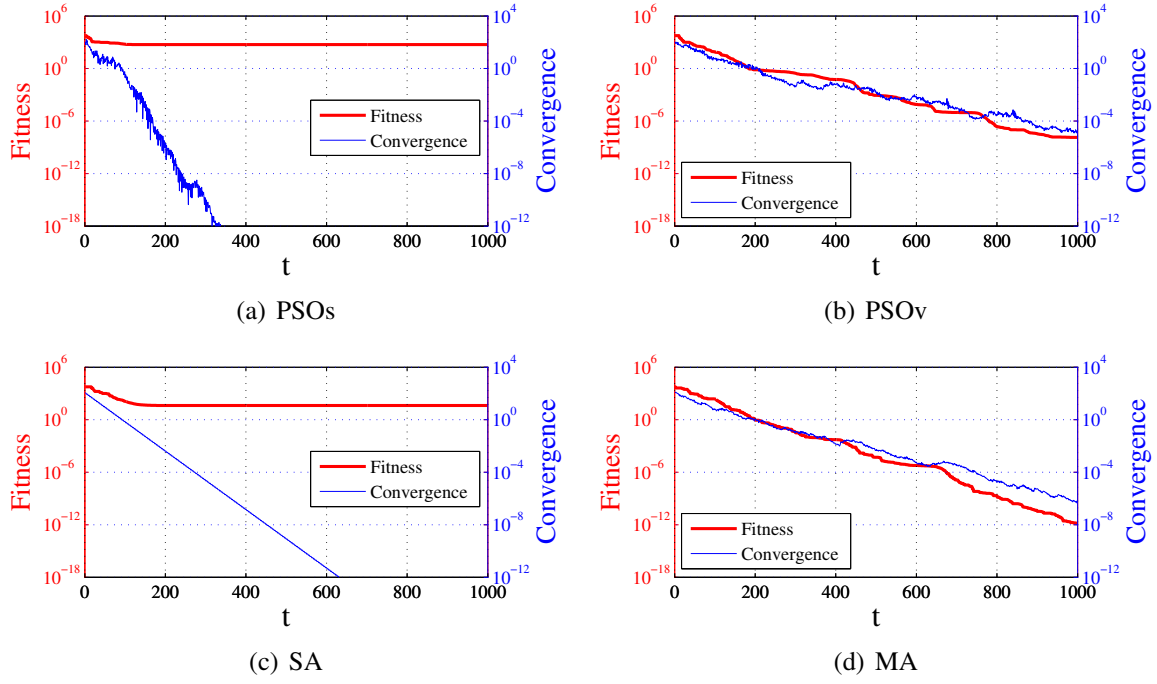


图 1.3: Search process of Rotated ellipsoidal function (f_2)

表 1.1: Results

| | f_1 Fitness | f_2 Fitness |
|------|---------------|---------------|
| PSOs | 5.26 E+02 | 6.67 E+02 |
| PSOv | 2.14 E-21 | 3.83 E-04 |
| SA | 1.63 E+00 | 7.14 E+01 |
| MA | 3.92 E-22 | 1.83 E-07 |

Namely, the behavior is caused by the random factor and the rotation angle. In general, we can say that the random factor leads to the diversity. On the other hand, our CD-PSO is a deterministic system, namely, the system does not contain the random factor. Even in such deterministic system, the CD-PSO can create the diversity to control the rotation angle.

This paper represents bias of the search and benchmark on the unimodal functions. Further studies are needed in order to analysis of the global search on the multimodal function.

第2章 PSO-based Multiple Optima Search Systems with Switched Topology

2.1 Introduction

The particle swarm optimization (PSO) is a meta-heuristic algorithm for solving optimization problems [4][5]. The particles represent potential solutions and move to find the target solutions according to its own and neighbors' history. The PSO is applicable to a variety of systems: neural networks, power electronics circuits [6][7], etc. This paper presents a novel PSO and considers its application to the multi-solution problems (MSP [6][13]) to find all the global minima of an objective function. The MSP is inevitable in practical/potential applications, therefore, several interesting methods have been studied [13]-[17]. This paper contains three points.

First, our PSO uses deterministic update of the particle position and velocity. The standard PSOs usually include stochastic parameters in the update and it is hard to analyze the convergence dynamics. Since the deterministic dynamical systems have strong analysis theory of the stability, several deterministic PSOs have been presented and their stability has been analyzed [8]. We have also proposed the canonical deterministic particle swarm optimization (CD-PSO) where the deterministic parameters are normalized and the dynamics is described by a canonical form equation [9][10][11]. The CD-PSO is convenient to grasp the effects of parameters on stability and dynamics.

Second, we consider the effects of the average distance (L_{avg}) of the swarm topology on the search capability. In the standard PSOs, the particle velocity depends on the best candidate solutions in the past history and all the particles know information of the best candidate. In other words, the swarm has network of fully connected topology. In this case, the particles tend to converge to one solution and are hard to find other solutions. In order to solve the MSP, it is important to delay the convergence and obstruct the transmission of information among the particles where the L_{avg} seems to be a vary important factor. We then investigate influence of the L_{avg} of several network structures (topology) upon the search capability in several examples. Especially, we introduce the switched topology and investigate its effects. In the switched topology, the information is not transmitted from the edge if the switch is off. The switching intervals relate virtually to the L_{avg} .

Third, we consider an application to analysis of the discrete dynamical systems (DDS). As a first step, we try to find multiple periodic points in two-dimensional DDS: it is one of the most basic problems to approach rich bifurcation phenomena. The problem is described as an MSP. . Performing numerical experiments for typical examples, the algorithm performance is investigated. There do not exist many works on application to DDS except for our works [17][18].

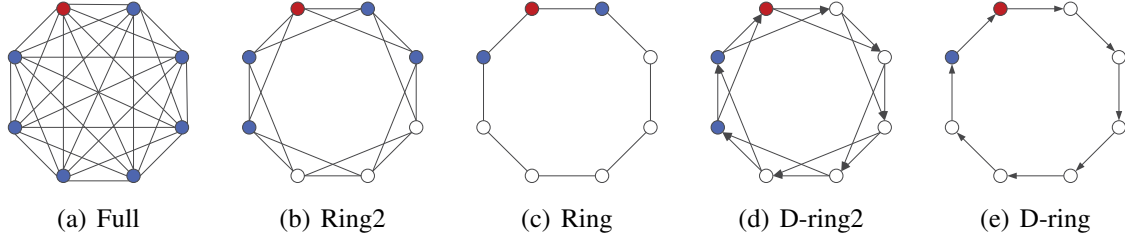


Fig 2.1: Network topology. Blue particles are neighbor of the red particle.

2.2 Particle swarm optimization

In this chapter, we derive the CD-PSO from the standard PSO.

2.2.1 Standard PSO

The standard PSO is described by

$$\begin{aligned} \mathbf{v}^n &\leftarrow w\mathbf{v}^n + c_1\mathbf{r}_1^n(\mathbf{Pbest}^n - \mathbf{x}^n) + c_2\mathbf{r}_2^n(\mathbf{Lbest}^n - \mathbf{x}^n) \\ \mathbf{x}^n &\leftarrow \mathbf{x}^n + \mathbf{v}^n \end{aligned} \quad (2.1)$$

where $\mathbf{x}^n = (x_1^n \dots x_D^n) \in \mathbb{R}^D$ denotes the location and $\mathbf{v}^n = (v_1^n \dots v_D^n) \in \mathbb{R}^D$ denotes the velocity, and n denote indices of particles. $\mathbf{Pbest}^n \in \mathbb{R}^D$ is called a personal best. It means the location that gives the best value of the evaluation function of the n -th particle in the past history. $\mathbf{Lbest}^n \in \mathbb{R}^D$ is called a local best. It means the location that gives the best value in neighborhood of the particle. The standard PSO has three parameters w , c_1 and c_2 . w is a weight coefficient. c_1 and c_2 are acceleration coefficients. $\mathbf{r}_1^n \in [0, 1]^D$ and $\mathbf{r}_2^n \in [0, 1]^D$ are independent uniform random numbers. We have adopted the parameter values recommended in Refs. [8] and [12].

$$\begin{cases} w = 0.729 \\ c_1 = c_2 = 1.49445 \end{cases} \quad (2.2)$$

Since Eq. (3.1) includes random numbers, we refer it as stochastic PSO hereafter.

2.2.2 Canonical Deterministic PSO

The CD-PSO can be derived from the stochastic PSO by omitting the stochastic factors. For simplicity we introduce the notation

$$\mathbf{p}^n = \gamma \mathbf{Pbest}^n + (1 - \gamma) \mathbf{Lbest}^n \quad (2.3)$$

$$\gamma = \frac{c_1}{c_1 + c_2}, \quad \mathbf{p}^n = (p_1^n \dots p_D^n) \quad (2.4)$$

where \mathbf{p}^n can be regarded as a desired fixed point, and means target location of searching. The parameter γ controls the mixture rate of the personal best and the local best. Since the variable component in each dimension is independent, we can consider one dimensional case

without loss of generality. Therefore, we consider one dimensional system hereafter. The one dimensional CD-PSO can be transformed into the following matrix form:

$$\begin{bmatrix} v_d^n \\ y_d^n \end{bmatrix} = \begin{bmatrix} \delta & -\omega \\ \omega & \delta \end{bmatrix} \begin{bmatrix} v_d^n \\ y_d^n \end{bmatrix} \quad (2.5)$$

where $y_d^n = x_d^n - p_d^n$. Note that this system does not include stochastic factors, therefore, this system is a deterministic system. The trajectory on the phase space rotates clockwise while the convergence. The dynamics of the CD-PSO is governed by the eigenvalues of the matrix in Eq. (2.5). The eigenvalues λ are given as

$$\lambda = \delta \pm j\omega \quad (2.6)$$

If λ are complex conjugate pairs, the system exhibits remarkable searching ability. Since this is a discrete-time system, the damping factor Δ and the rotation angle θ on each iteration can be derived by the complex eigenvalues as

$$\Delta = \sqrt{\delta^2 + \omega^2} \quad (2.7)$$

$$\theta = \arctan \frac{\omega}{\delta} \quad (2.8)$$

If the damping factor satisfies the condition $0 < \Delta < 1$ then the system is said to be stable. Based on the above discussion, the CD-PSO is described as

$$\begin{bmatrix} x_d^n \\ v_d^n \end{bmatrix} = \Delta \begin{bmatrix} \cos \theta_d^n & -\sin \theta_d^n \\ \sin \theta_d^n & \cos \theta_d^n \end{bmatrix} \begin{bmatrix} x_d^n - p_d^n \\ v_d^n \end{bmatrix} + \begin{bmatrix} p_d^n \\ 0 \end{bmatrix} \quad (2.9)$$

where target location $p_d^n \equiv \mathbf{Lbest}^n$ corresponds to $\gamma = 0$. The CD-PSO has two parameters Δ and θ_d^n . The parameter Δ is a damping factor that controls convergence of particles. θ_d^n is a rotation angle that controls the frequency and sampling interval of the search.

We determine the rotation angle θ_d^n as follows:

$$\theta_d^n = [\{ (n-1)D + d \} \phi] \bmod 360^\circ \quad (2.10)$$

where ϕ is basis angle. In the cases of $D=3$ and $N=10$, the parameters are as follows:

$$\begin{bmatrix} \theta_1^1 & \theta_2^1 & \theta_3^1 \\ \theta_1^2 & \theta_2^2 & \theta_3^2 \\ \vdots & & \\ \theta_1^{10} & \theta_2^{10} & \theta_3^{10} \end{bmatrix} = \begin{bmatrix} \phi & 2\phi & 3\phi \\ 4\phi & 5\phi & 6\phi \\ \vdots & & \\ 28\phi & 29\phi & 30\phi \end{bmatrix}$$

Based on our preliminary experimental results, the parameters are determined as

$$\begin{cases} \Delta = 0.98 \\ \phi = 180(3 - \sqrt{5}) = 137.51^\circ \end{cases} \quad (2.11)$$

The value adopted in ϕ is the golden angle that often appears in nature and is known as a suitable angle to fill the circle.

2.3 Topology of network structure

For the stochastic PSO, the location information which gives the best value of the evaluation function is shared with the other particles in the swarm. On the other hand, there is the case where the best information is given within a subset in the whole swarm. In such a case, the best information is called as a local best \mathbf{Lbest}^n . How to get the local best information from any population is equivalent to construct a network structure. Namely, the population corresponds to the connection relations which can be expressed as network topology in the graph theory. Such a network structure influences the performance of searching capability. Therefore, we analyze a relationship between network structures of swarm and the performance by using graph theory of features.

We use the average distance L_{avg} and the number of edges M in the graph theory as measures to evaluate the topology. The distance between two vertices in a graph is the number of edges in the shortest path connecting them. The average distance L_{avg} means its average and is described as

$$L_{\text{avg}} = \frac{1}{N(N-1)} \sum_m \sum_{m \neq n} r_{mn} \quad (2.12)$$

where N denotes the number of particles, and r_{mn} represents the distance between the m -th and n -th particles.

2.3.1 Undirected topology

In order to compare the effects of the topology, we consider some examples as illustrated in Fig. 3.2 (a)-(c): fully connected mesh topology (Full), ring network topology (Ring) and extended ring topology of adjacent two vertices apart (Ring2). We have carried out the following numerical simulations with these topologies of the CD-PSO. In order to confirm the performance, Himmelblau function is used as a benchmark function. The function is described as the following:

$$f_{\text{Himmelblau}}(\mathbf{x}) = (x_1^2 + x_2 - 11)^2 + (x_1 + x_2^2 - 7)^2 \quad (2.13)$$

where $\mathbf{x} = (x_1, x_2)^T \in [-6, 6]^2$. This function has 4 global optima (solutions) as illustrated in Fig. 2.2. The criterion for successful search is $f_{\text{Himmelblau}}(\mathbf{x}) < 0.01$. The experimental conditions are summarized in Table 3.3. We measure the success rate (SR) in average of 10 trials. Each trial is calculated 200 times with different initial values. The initial values are given from uniform random numbers with ranges $x_d^n \in [-6, 6]$ and $v_d^n \in [-6, 6]$. The results are summarized in Table 2.2. The SR tends to be improved as L_{avg} increases and M decreases.

2.3.2 Directed topology

In order to increase the L_{avg} , a directed graph is applied to our system. In general, topologies used in PSO are undirected graph. However it is easy to convert undirected graph into directed graph. In this paper, we consider a directed ring topology (D-ring) and a directed extended ring topology (D-ring2) as shown in Figs. 3.2 (d) and (e). We have carried out

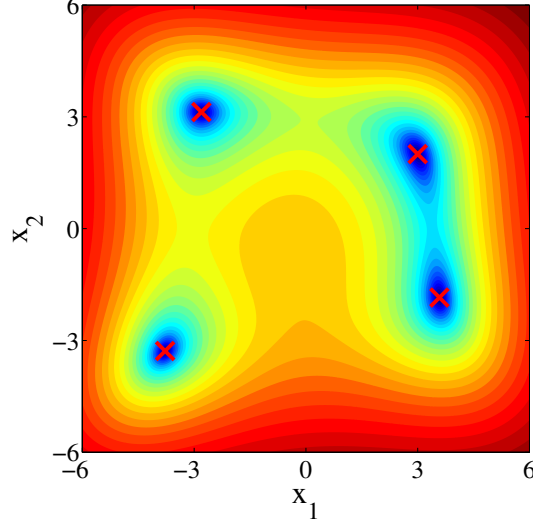


图 2.2: Contour map of the Himmelblau function where colder color denotes lower height. The red crosses denote the multi-solution.

表 2.1: Parameter configuration for the benchmark problem

| | |
|-----------------------------|-----------------|
| swarm's size N | 40 |
| damping factor Δ | 0.98 |
| rotation angle θ_d^n | Eq. (3.5)(3.6) |
| maximum iteration | 800 |
| trial number | 200×10 |

similar numerical simulations to confirm effects of the directed graph. The results are summarized in Table 2.3. The directed topology has longer average distance than the undirected graph topology. The experimental results indicate that the directed graph topology improves the SR. This fact suggests that the long average distance leads to the improved SR.

表 2.2: Undirected topology

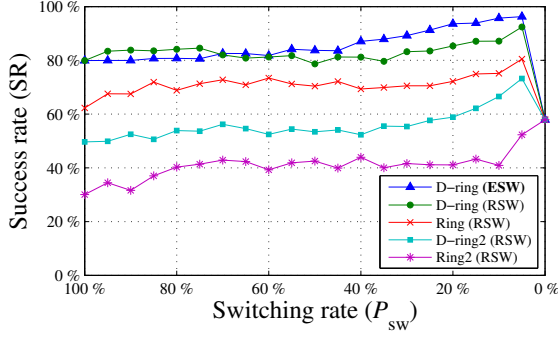
| topology | Full | Ring2 | Ring |
|-----------|------|-------|------|
| L_{avg} | 1.0 | 5.4 | 10.3 |
| M | 780 | 80 | 40 |
| degree | 39 | 4 | 2 |
| SR | 0% | 30% | 62% |

2.4 Switched topology

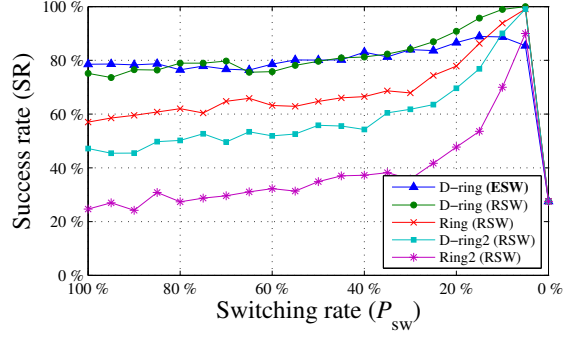
In order to increase the L_{avg} further, we introduce the switched topology. We apply the switches to the edges. The switch-off means that the corresponding edge is unconnected.

表 2.3: Directed topology

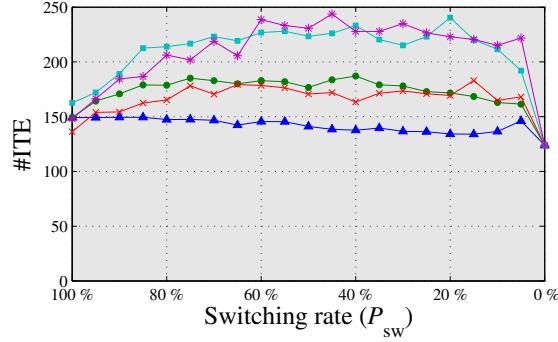
| topology | D-ring2 | D-ring |
|-----------|---------|--------|
| L_{avg} | 10.3 | 20.0 |
| M | 80 | 40 |
| indegree | 2 | 1 |
| SR | 50% | 80% |



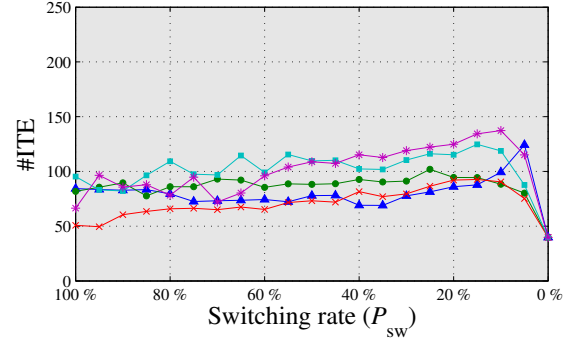
(a) CD-PSO



(b) Stochastic PSO



(c) CD-PSO



(d) Stochastic PSO

图 2.3: Result of Himmelblau function

The switch-on means that the edges are connected. The number of switches is equal to the number of edges M . When the switch is off, the information is not transmitted between the edges.

2.4.1 Random switching

As a rule of the switch, we apply the random switching rule (RSW). In RSW, k switches are turned on depending on uniform random numbers. We defined switching rate $P_{sw} = k/M$. Figure 2.4 (a) shows example of a case of $M = 4$, $k = 1$. Namely P_{sw} is equal to 0.25 shown in Fig.2.4 (b).

We have carried out similar numerical simulations to confirm effects of the switched topology using RSW. The results of SR are summarized in Fig. 2.3 (a). Note that the case of

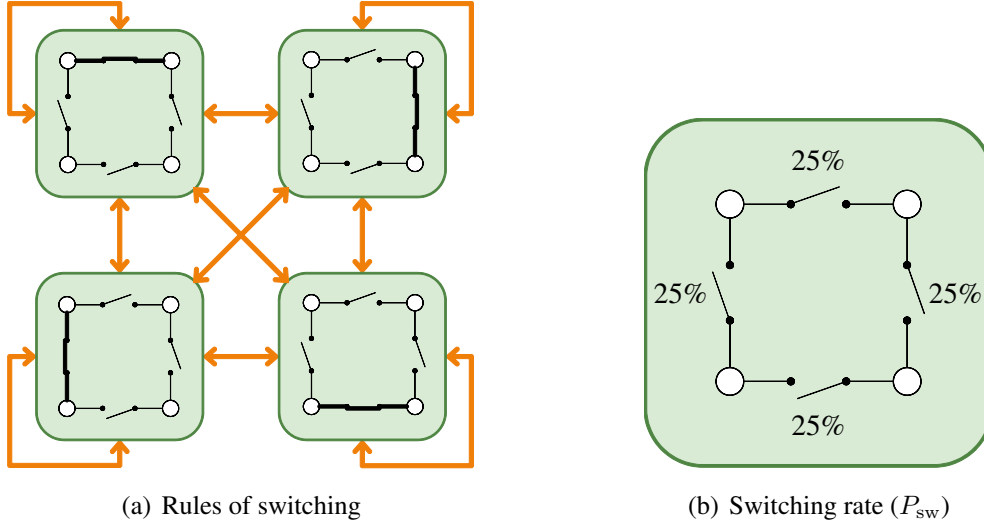


Fig. 2.4: Switched topology

$P_{sw} = 100\%$ equals to normal topology without switching. The case of $P_{sw} = 0\%$ means each particle is isolated, thus, it refers to its own information only. The experimental results indicate that smaller P_{sw} leads to the improved SR. In smaller P_{sw} , almost all the switches are turned off and transmission of information is difficult. Hence it ought to increase L_{avg} when P_{sw} decreases. The long L_{avg} seems to be effective.

The results of #ITE are summarized in Fig. 2.3 (c), where #ITE denotes the average number of iterations to attain the criterion. It measures search speed. The experimental results show that the #ITE has a peak of around $P_{sw} = 50\%$.

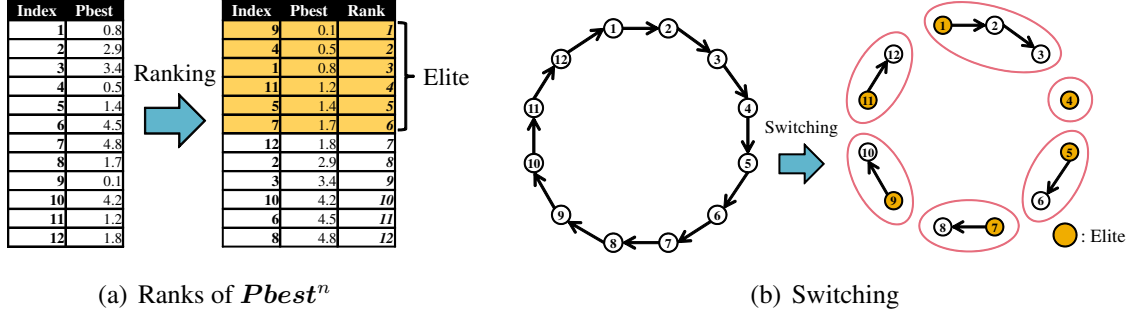
2.4.2 Elite preservation switching

The RSW is a stochastic switching rule and does not consider the state of the particles. In this chapter, we introduce a deterministic switching rule applying the concept of elite preservation strategy. Elite preservation strategy is used in genetic algorithms and it preserves a superior individual preferentially. In the PSO, the particle which has a good P_{best}^n , can be regarded as an elite. Elite preservation switching (ESW) is preferentially detached from the connected edge. In order to separate the elite effectively, we apply a D-ring topology. The ESW is defined as the following. First, determine the elite by ranks of P_{best}^n as shown in Fig.2.5 (a). Second, turn off the switch that connects to the elite as shown in Fig.2.5 (b). The elite particles are separated from other elites by the ESW.

We have carried out similar numerical simulations using the ESW. The results are illustrated in Figs. 2.3 (a) and (c), where P_{sw} is calculated by the rate of the elites in the swarm. The ESW procedure exhibits the highest SR and the fastest #ITE. It should be emphasized that the CD-PSO using the ESW is a completely deterministic system.

2.4.3 Comparison with the stochastic PSO

We have used the CD-PSO for analyze to effects of the topology without stochastic factors. In this chapter, we compare the conventional stochastic PSO in Eq. (3.1) with the CD-PSO.



☒ 2.5: Elite preservation switching

We have carried out the same numerical simulations using stochastic PSO with parameters in Eq. (2.2). The results are illustrated in Figs. 2.3 (b) and (d). The experimental results indicate that the long average distance and smaller P_{sw} lead to the improved SR. This trend is similar to the CD-PSO. However, when the ESW is applied to the stochastic PSO, the search performance is not improved as compared with the CD-PSO.

The stochastic PSO has a random number parameter r_2^n . If $r_2^n = 0$, it does not use $Lbest^n$ to move the particles. This is equivalent to switch off in topology. The stochastic PSO is difficult to analyze, because random number parameters affect the topology.

2.4.4 Summary of experimental results

The above experimental results can be summarized as follows:

- A The longer L_{avg} leads to the improved SR.
- B The smaller P_{sw} , which is interpreted as longer L_{avg} , leads to the improved SR.
- C The CD-PSO with ESW is a complete deterministic system that can realize high SR and small #ITE.

2.5 Exploring periodic points of dynamical systems

In this chapter, we apply the CD-PSO to exploring periodic points of dynamical systems. For simplicity, we consider the 2-dimensional system (2D map) described by

$$\mathbf{x}(t+1) = \mathbf{F}(\mathbf{x}(t)) : \begin{cases} x_1(t+1) = F_1(x_1(t), x_2(t)) \\ x_2(t+1) = F_2(x_1(t), x_2(t)) \end{cases} \quad (2.14)$$

where t is a discrete time. A point \mathbf{Q} is said to be a T -periodic points if $\mathbf{F}^T(\mathbf{Q}) = \mathbf{Q}$, $\mathbf{F}^k(\mathbf{Q}) \neq \mathbf{Q}$ for $0 < k < T$, where \mathbf{F}^T is the T -fold composition of \mathbf{F} . A 1-periodic point is referred to as a fixed point. We consider exploring T -periodic points. It is basic to analyze bifurcation phenomena of the dynamical systems. The evaluation function is defined by

$$f_T(x_1(t), x_2(t)) = \left\{ F_1^T(x_1(t), x_2(t)) - x_1(t) \right\}^2 + \left\{ F_2^T(x_1(t), x_2(t)) - x_2(t) \right\}^2 \quad (2.15)$$

It is nonnegative function that becomes 0 if $[x_1(t), x_2(t)]$ is a T -periodic or T' -periodic point, where T' is the divisor of T . We explore periodic points on two well-known 2D maps.

Ikeda map

$$\begin{cases} F_1[x_1(t), x_2(t)] = u(x_1 \cos \tau - x_2 \sin \tau) + 1 \\ F_2[x_1(t), x_2(t)] = u(x_1 \sin \tau + x_2 \cos \tau) \end{cases} \quad (2.16)$$

$$\tau = 0.4 - \frac{6}{1+x_1^2+x_2^2}$$

where $(x_1(t), x_2(t))^T \in [-2.5, 4.5]^2$ and $u = 0.9$. Substituting Eq. (2.16) with $T = 1$ and $T = 2$ into Eq. (2.15), we obtain the evaluation function f_{Ikeda1} and f_{Ikeda2} , respectively.

Henon map

$$\begin{cases} F_1[x_1(t), x_2(t)] = \cos \alpha x_1 - \sin \alpha (x_2 - x_1^2) \\ F_2[x_1(t), x_2(t)] = \sin \alpha x_1 + \cos \alpha (x_2 - x_1^2) \end{cases} \quad (2.17)$$

where $(x_1(t), x_2(t))^T \in [-1, 1]^2$ and $\cos \alpha = 0.24$. Substituting Eq. (2.17) with $T = 5$ into Eq. (2.15), we obtain the evaluation function f_{Henon5} .

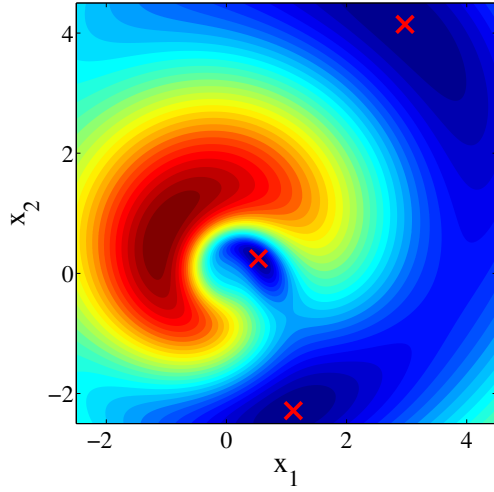
表 2.4: Condition of periodic points search

| evaluation function | f_{Ikeda1} | f_{Ikeda2} | f_{Henon5} |
|---------------------------|---------------------|---------------------|---------------------|
| the number of optima | 3 | 5 | 11 |
| initial location | $[-2.5, 4.5]^2$ | $[-2.5, 4.5]^2$ | $[-1, 1]^2$ |
| initial velocity | $[-3.5, 3.5]^2$ | $[-3.5, 3.5]^2$ | $[-1, 1]^2$ |
| the criterion for success | 0.01 | 0.005 | 0.0001 |

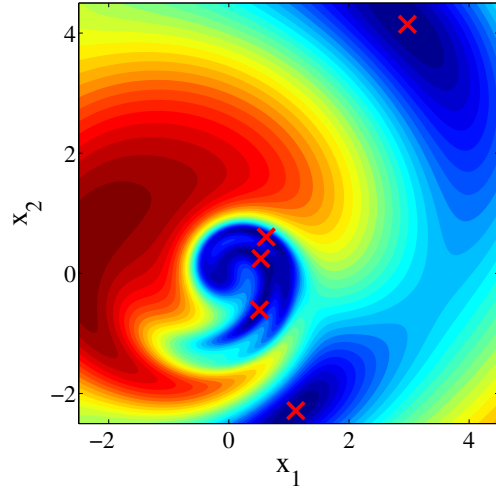
Figure 3.4 shows contour maps of these evaluation functions where the red crosses denote the periodic points, the target multi-solution. We have carried out the same numerical simulations using evaluation function of each mapping. The other experimental conditions are summarized in Table 2.4. The simulation results are shown in Figs. 2.7, 2.8, and 2.9. We can see similar trend to A to C in section 2.4.4. However, the CD-PSO with ESW of f_{Henon5} gives lower SR than other problems. It requires further analysis.

2.6 Conclusions

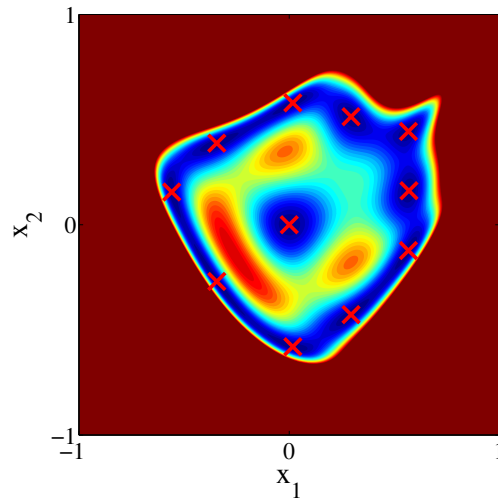
Effects of topology in a multiple optima search have been discussed in this paper. A directed graph is applied to the topology, and it is shown that the SR tends to be improved as the average distance increases. We have then considered the switched topology. The simulation results indicate that smaller switching rate leads to the improved SR. The result indicates frequent transmission of information is not necessary. This characteristic is effective in parallel computing. Since switched topology is disconnected, the average distance cannot be calculated. It is future problems to quantify distance using the switching rate.



(a) f_{Ikeda1} for fixed points of the Ikeda map.

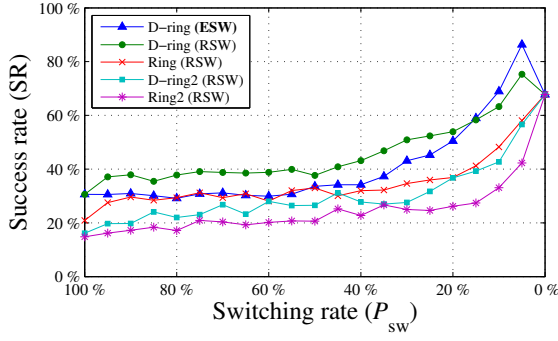


(b) f_{Ikeda2} for 2-periodic points and fixed points of the Ikeda map.

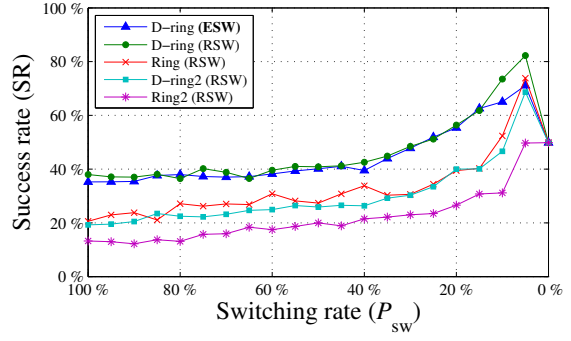


(c) f_{Henon5} for 5-periodic points and fixed point of Henon map.

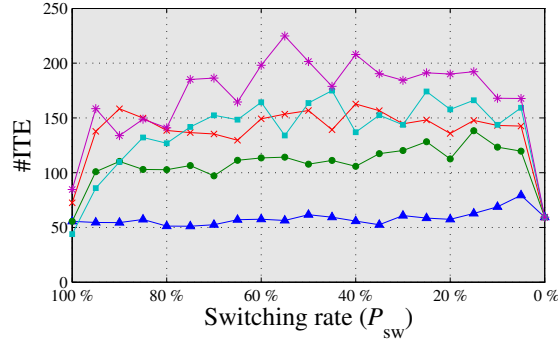
☒ 2.6: Contour maps of the evaluation functions where colder color denotes lower height.



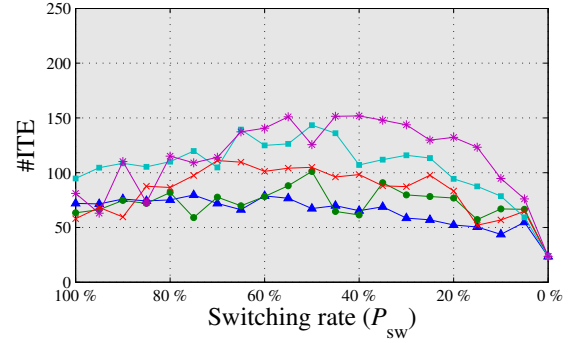
(a) CD-PSO



(b) Stochastic PSO

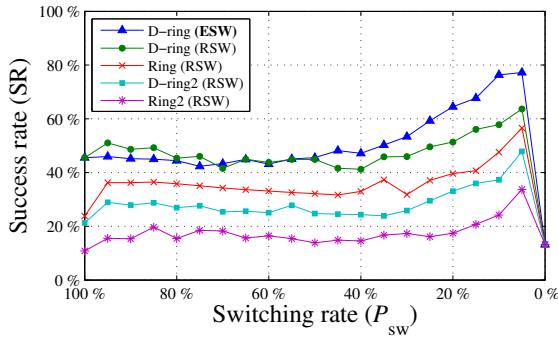


(c) CD-PSO

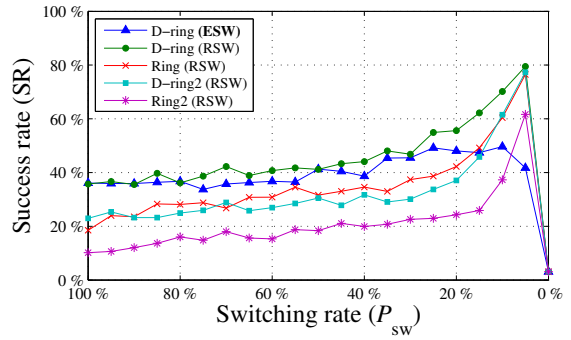


(d) Stochastic PSO

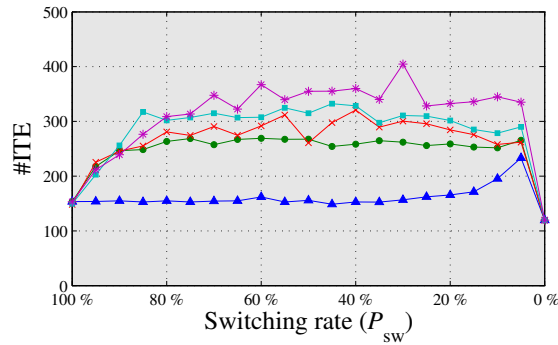
⊠ 2.7: f_{Ikeda1} for fixed points of the Ikeda map.



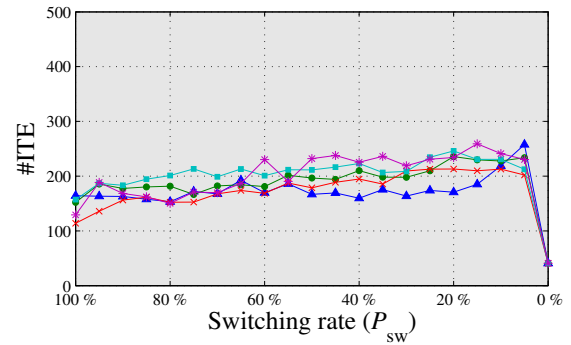
(a) CD-PSO



(b) Stochastic PSO

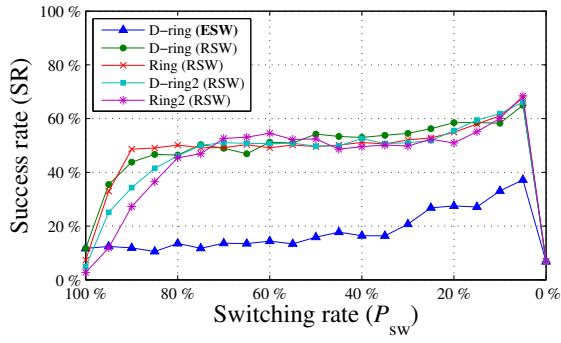


(c) CD-PSO

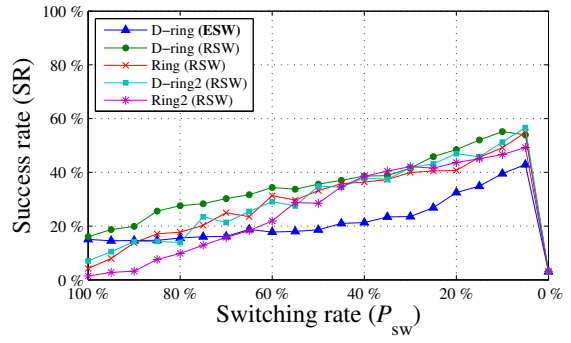


(d) Stochastic PSO

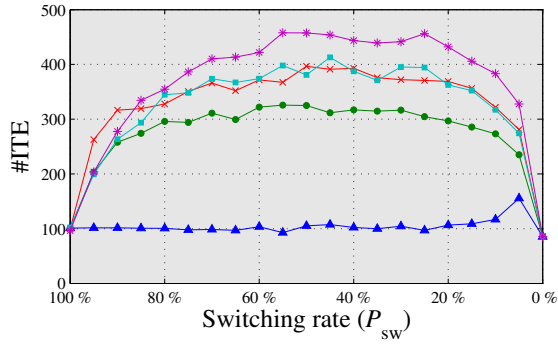
⊠ 2.8: f_{Ikeda2} for 2-periodic points and fixed points of the Ikeda map.



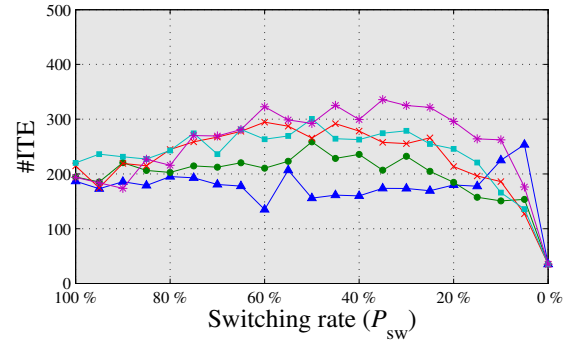
(a) CD-PSO



(b) Stochastic PSO



(c) CD-PSO



(d) Stochastic PSO

Figure 2.9: f_{Henon5} for 5-periodic points and fixed point of Henon map.

第3章 Particle Swarm Optimization with Switched Topology and Deterministic Parameters

3.1 Introduction

The particle swarm optimization (PSO) is a population-based optimization algorithm inspired by flocking behavior of living beings [4][5]. The PSO is simple in concept, is easy to implement and can search feasible solutions without gradient information of the evaluation function. The PSO has been applied to design of various systems [6] including neural networks [19], power electrical circuits [7][20] and discrete dynamical systems [18]. The PSO consists with particles which move to find solution(s) in the search space. Each particle memorizes own best location which represents a feasible solution. Such own best location is called as *Pbest*. Another best information is selected from a limited population, and the best information is called as *Lbest*. Each particle determines the direction of movement using *Pbest* and *Lbest*. The conventional PSO contains random parameters and can be regarded as a stochastic system. Thus, the theoretical analysis of the dynamics of the conventional PSO is pretty difficult.

In order to improve the PSO performance, this paper studies PSO with switched topology and deterministic parameters. The proposed PSO does not include stochastic parameters and is suitable for theoretical analysis. The switched topology can give flexibility to determine the *Lbest*. If the *Lbest* information is selected from all the particles, the corresponding network can be regarded as a complete graph. There are a variety of network topologies to be represented in the complex network [21]. In order to clarify the relationship between the network topology and the searching performance, the average distance of the network is a basic measure [11]. In graph theory, the distance between two vertices is the number of the edges in a shortest path connecting them. Roughly speaking, longer average distance tends to give better search performance [11]. For example, the ring topology gives longer average distance than complete graph. Moreover, the directed graph structure gives the longer average distance than the undirected graph. In order to prolong the average distance, we introduce the switched topology to the link. The switched topology is a dynamic topology to change a connection structure depending on the state of switches. In order to characterize the switched topology, we propose an index to measure the feature of the graph. The index is a switching distance that corresponds to the average distance in usual graph. Based on the switching distance, we investigate the search performance. We then apply the PSO with switched topology to the multi-solution problems (MSPs [2][6][13]). The purpose of the MSP is to find all global minima of an objective function. The MSP is inevitable in practical problems and various algorithms have been discussed [13]-[17]. We have carried out numerical simulations to confirm the effect of the switching topology by using well-known benchmark functions of the MSP.

Note that [2] has presented the switched topology, however, it does not discuss the switch-

ing distance and numerical simulation of typical benchmarks.

3.2 Particle swarm optimization

In this section, we introduce a canonical deterministic PSO (CD-PSO).

3.2.1 Standard PSO

The conventional particle swarm optimization system contains stochastic factors and we call it the standard PSO. In order to analyze the dynamics theoretically, and to implement the system by an electronics circuit, we proposed a canonical deterministic PSO [9][10]. The canonical deterministic PSO (CD-PSO) is based on the standard PSO [4][5]. Therefore, as a preparation to introduce the CD-PSO, we summarize the standard PSO. The standard PSO is described by

$$\begin{aligned} \mathbf{v}^n &\leftarrow w\mathbf{v}^n + c_1\mathbf{r}_1^n(\mathbf{Pbest}^n - \mathbf{x}^n) + c_2\mathbf{r}_2^n(\mathbf{Lbest}^n - \mathbf{x}^n) \\ \mathbf{x}^n &\leftarrow \mathbf{x}^n + \mathbf{v}^n \end{aligned} \quad (3.1)$$

where $\mathbf{x}^n = (x_1^n \dots x_D^n) \in \mathbb{R}^D$ denotes a location of particle, $\mathbf{v}^n = (v_1^n \dots v_D^n) \in \mathbb{R}^D$ denotes its velocity, and n denotes an index of particle. $\mathbf{Pbest}^n \in \mathbb{R}^D$ is called as a personal best. It means the location that gives the best value of the evaluation function of the n -th particle in the past history. $\mathbf{Lbest}^n \in \mathbb{R}^D$ is called as a local best. It means the location that gives the best value in the neighborhood of the n -th particle. The standard PSO has three parameters w , c_1 and c_2 . w is an inertia coefficient. c_1 and c_2 are acceleration coefficients. $\mathbf{r}_1^n \in [0, 1]^D$ and $\mathbf{r}_2^n \in [0, 1]^D$ are independent uniform random numbers. If a PSO includes a random parameter, we refer it as a stochastic PSO hereafter.

3.2.2 Canonical Deterministic PSO

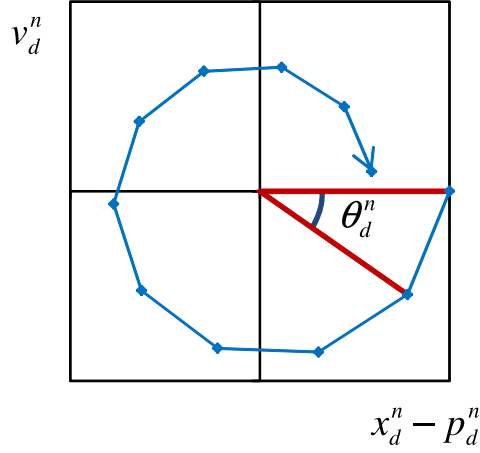
The CD-PSO can be derived from the stochastic PSO by omitting the stochastic factors. For simplicity, we introduce the following notations.

$$\mathbf{p}^n = \gamma\mathbf{Pbest}^n + (1 - \gamma)\mathbf{Lbest}^n \quad (3.2)$$

$$\gamma = \frac{c_1}{c_1 + c_2}, \quad \mathbf{p}^n = (p_1^n \dots p_D^n) \quad (3.3)$$

where \mathbf{p}^n can be regarded as a desired fixed point, and means a target location of searching. The parameter γ controls the mixture rate between the personal best and the local best. In this paper, we consider the case where $\gamma = 0$, namely, the desired fixed point corresponds to the local best of each particle. Since the variable component in each dimension is independent, we can consider one dimensional case without loss of generality. Therefore, we consider one dimensional system hereafter. The one dimensional CD-PSO is described by the following matrix form [9][10].

$$\begin{bmatrix} x_d^n \\ v_d^n \end{bmatrix} = \Delta \begin{bmatrix} \cos \theta_d^n & -\sin \theta_d^n \\ \sin \theta_d^n & \cos \theta_d^n \end{bmatrix} \begin{bmatrix} x_d^n - p_d^n \\ v_d^n \end{bmatrix} + \begin{bmatrix} p_d^n \\ 0 \end{bmatrix} \quad (3.4)$$



⊠ 3.1: The trajectory of the CD-PSO in the phase space

where target location is $p_d^n \equiv \mathbf{Lbest}^n$. Note that this system does not include stochastic factors, therefore, this system can be regarded as a deterministic system. The CD-PSO has two parameters Δ and θ_d^n . The parameter Δ is a damping factor that controls convergence speed of particles. θ_d^n denotes a rotation angle that controls the sampling interval of the search. If the damping factor Δ satisfies the condition $0 < |\Delta| < 1$, the system is said to be a stable and the trajectory on the phase space converges to the fixed point while rotating clockwise as shown in Fig. 3.1.

We determine the rotation angle θ_d^n as follows:

$$\theta_d^n = [\{ (n-1)D + d \} \phi] \bmod 360^\circ \quad (3.5)$$

where ϕ is a basis angle. In the case of $D=3$ and $N=10$, the parameters are set as follows:

$$\begin{bmatrix} \theta_1^1 & \theta_2^1 & \theta_3^1 \\ \theta_1^2 & \theta_2^2 & \theta_3^2 \\ \vdots & & \\ \theta_1^{10} & \theta_2^{10} & \theta_3^{10} \end{bmatrix} = \begin{bmatrix} \phi & 2\phi & 3\phi \\ 4\phi & 5\phi & 6\phi \\ \vdots & & \\ 28\phi & 29\phi & 30\phi \end{bmatrix}$$

Based on our preliminary experimental results [1], the parameters are determined as

$$\begin{cases} \Delta = 0.98 \\ \phi = 180(3 - \sqrt{5}) = 137.51^\circ \end{cases} \quad (3.6)$$

The applied rotation angle is called as the golden angle. The golden angle often appears in nature and is known as a suitable angle to fill the circle. By using the golden angle, we expect that the CD-PSO is to explore the various points.

3.3 Topology of network structure

In exploring, PSO's particles move toward the known location which gives the best value of the evaluation function. The location information is shared with the other particles in the swarm. Structure of information sharing among the particles can be represented by a

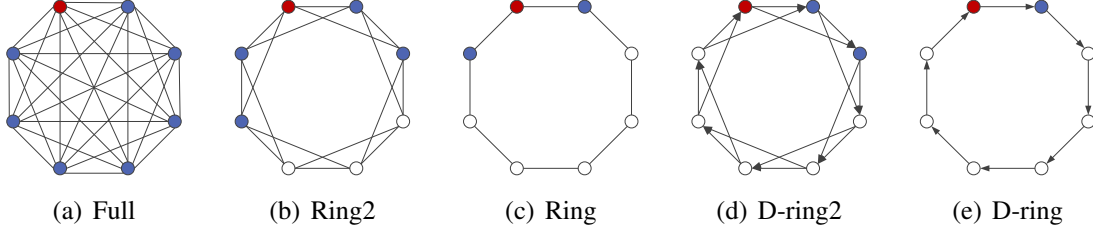


Fig. 3.2: Network topologies. Blue particles are neighbor of the red particle.

topology of network. Figure 3.2 shows the typical topologies. In standard PSO, the global best (G_{best}) is applied, which is the known best location in the swarm. In other words all the particles know all other particle's information of the swarm. Namely, the standard PSO uses fully connected topology as shown in Fig. 3.2(a). In this case, the best information is easily transmitted and all the particles converge into G_{best} speedily. However, it can explore only one solution and tends to trap into local solutions.

In other case, PSO also uses L_{best} , which treats the best information within a limited population. For example, in the limited population as shown in Fig. 3.2(c), each particle is connected to the both sides' particles. State of the exchange of the best information can be expressed as a graph in this way. In this case, the PSO uses ring connected topology as shown in Fig. 3.2(c). Comparing with the full connection, the transmission speed of the best information of the ring topology is said to be slow. Namely, the information transmission speed is depended on the characteristic of the graph which corresponds to the network structure. Thus we pay attention to the average distance of the graph. For simplicity, we consider the PSO has regular network topologies in this paper. Each node of the regular network topologies has the same number of links exactly. Figure 3.2 illustrates the examples of objective regular network topologies. Figures 3.2(a), (b) and (c) are undirected network topologies, namely, complete graph, extended circle graph, and circle graph, respectively. Figures 3.2(d) and (e) are directed extended circle graph and directed circle graph, respectively.

3.3.1 Average distance

The average distance L is said to be a measure of difficulty of information transmission for topology. The L is defined by the following equation:

$$L = \frac{1}{N(N-1)} \sum_m \sum_{m \neq n} l_{mn} \quad (3.7)$$

where N denotes the number of particles, and l_{mn} represents the distance between the m -th and n -th particles. Table 3.1 represents the calculation results of each topology, where M is the number of edges and indegree is the number of edges directed into a vertex in a directed graph. We have reported that the longer L leads to the improved exploring [11].

3.4 Switched topology

In the regular network topologies, the directed ring topology has the longest average distance. In order to increase the average distance L further, we introduce the switched topology.

表 3.1: The basic data of topologies in the case of 20 particles

| Topology | Full | Ring2 | Ring | D-ring2 | D-ring |
|----------|------|-------|------|---------|--------|
| L | 1.00 | 2.89 | 5.26 | 5.26 | 10.0 |
| M | 190 | 40 | 20 | 40 | 20 |
| indegree | 19 | 4 | 2 | 2 | 1 |

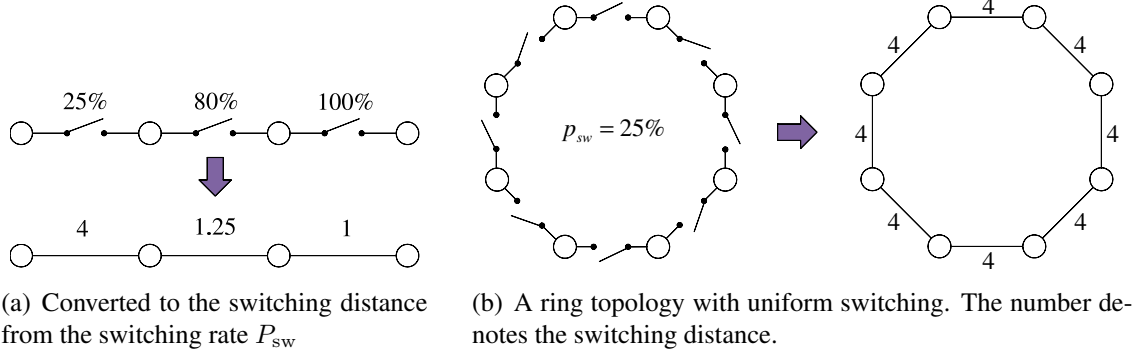


图 3.3: Switching distance

ogy. We apply the switches to the edges. The switch-off means that the corresponding edge is unconnected. The switch-on means that the edge is connected. The number of switches is equal to the number of edges M . When the switch is off, the information is not transmitted between the nodes. This operation can realize similar effects to increase the average distance.

3.4.1 Switching rate

We assume that the average distance is depend on the switching rule. Although there are various switching rules, we apply the random switching rule (RSW), which is k switches are turned on depending on uniform random numbers. We defined switching rate $P_{sw} = k/M$. Note that the case of $P_{sw} = 100\%$ equals to normal topology without switching. The case of $P_{sw} = 0\%$ means all particles are isolated, thus, they refer to their own information only.

3.4.2 Switching distance

In order to quantify *distance* in switched topology, we introduce a switching distance L_{sw} . The switching distance L_{sw} is given by a reciprocal number of the P_{sw} as shown in Fig. 3.3(a). For example, in the case of $P_{sw} = 25\%$, the switching distance is $1/0.25 = 4$ where the switch turns on once in four times. In the case of $P_{sw} = 100\%$, the switching distance is 1 and equals to normal topology. Figure 3.3(b) shows the switched ring topology with $P_{sw} = 25\%$ constant. In this case, since the network is a regular network, the switching distance is calculated as follows.

$$L_{sw} = L \cdot \frac{1}{P_{sw}} \quad (3.8)$$

We adopt the random switching for topology of Fig. 3.2 hereafter.

表 3.2: Benchmark functions

| Function | Domain of \mathbf{x} | Optimal value | The number of solutions | The criterion for successful |
|---|------------------------|---------------|-------------------------|------------------------------|
| $f_1(\mathbf{x}) = (x_2 - \frac{5.1}{4\pi^2}x_1^2 + \frac{5}{\pi}x_1 - 6)^2 + 10(1 - \frac{1}{8\pi})\cos(x_1) + 10$ | $[-5, 15]^2$ | 0 | 3 | 0.05 |
| $f_2(\mathbf{x}) = (x_1^2 + x_2 - 11)^2 + (x_1 + x_2^2 - 7)^2$ | $[-6, 6]^2$ | 0 | 4 | 0.05 |
| $f_3(\mathbf{x}) = 2 - \cos(\pi x_1) + \cos(\frac{1}{2}\pi x_2)$ | $[-3, 3]^2$ | 0 | 6 | 0.01 |
| $f_4(\mathbf{x}) = \sum_{i=1}^5 i \cos[(i+1)x_1 + i] \cdot \sum_{i=1}^5 i \cos[(i+1)x_2 + i] + 186.731$ | $[-4, 8]^2$ | 0 | 8 | 20 |

3.5 Simulation

In order to clarify a relationship between the switched topology and its searching performance, we carry out some numerical simulations by using benchmark functions as shown in Table 3.2. These functions are called that $f_1(\mathbf{x})$ is Branin, $f_2(\mathbf{x})$ is Himmelblau and $f_4(\mathbf{x})$ is Shubert. These functions are well-known benchmark functions of the MSPs [22]-[24]. (However $f_3(\mathbf{x})$ is an original function of this paper.) Thus, these functions have plural optimal solutions. Contour of the benchmark functions are illustrated in Fig. 3.4. In these figures, the cross-mark (\times) denotes an optimal point. The purpose of these numerical simulations is to find all the optimal solutions of an objective function. The experimental conditions are summarized in Table 3.3. We measure the average of the number of found optimal solutions (#SOL). Each trial is calculated with different initial values of \mathbf{x}^n and \mathbf{v}^n . The initial values are set by uniform random numbers.

3.5.1 Search process

Figures 3.5 and 3.6 illustrate search process of the normal ($P_{\text{sw}} = 1.0$) and the switched ($P_{\text{sw}} = 0.25$) ring topologies in $f_2(\mathbf{x})$, respectively. Since the information transmission of the normal ring topology is faster than that of the switched ring topology, particles of the normal ring topology tend to be attracted to the other solutions. However, in the switched ring topology, the information transmission is often cut off. Consequently, the information transmission speed of the switched ring topology seems to be slow. Hence particles are not attracted and are able to find many solutions.

表 3.3: Parameter configuration for the benchmark problems

| | |
|-----------------------------|-----------------|
| swarm's size N | 20 |
| damping factor Δ | 0.98 |
| rotation angle θ_d^n | Eqs. (3.5)(3.6) |
| maximum iteration | 1000 |
| trial number | 4000 |

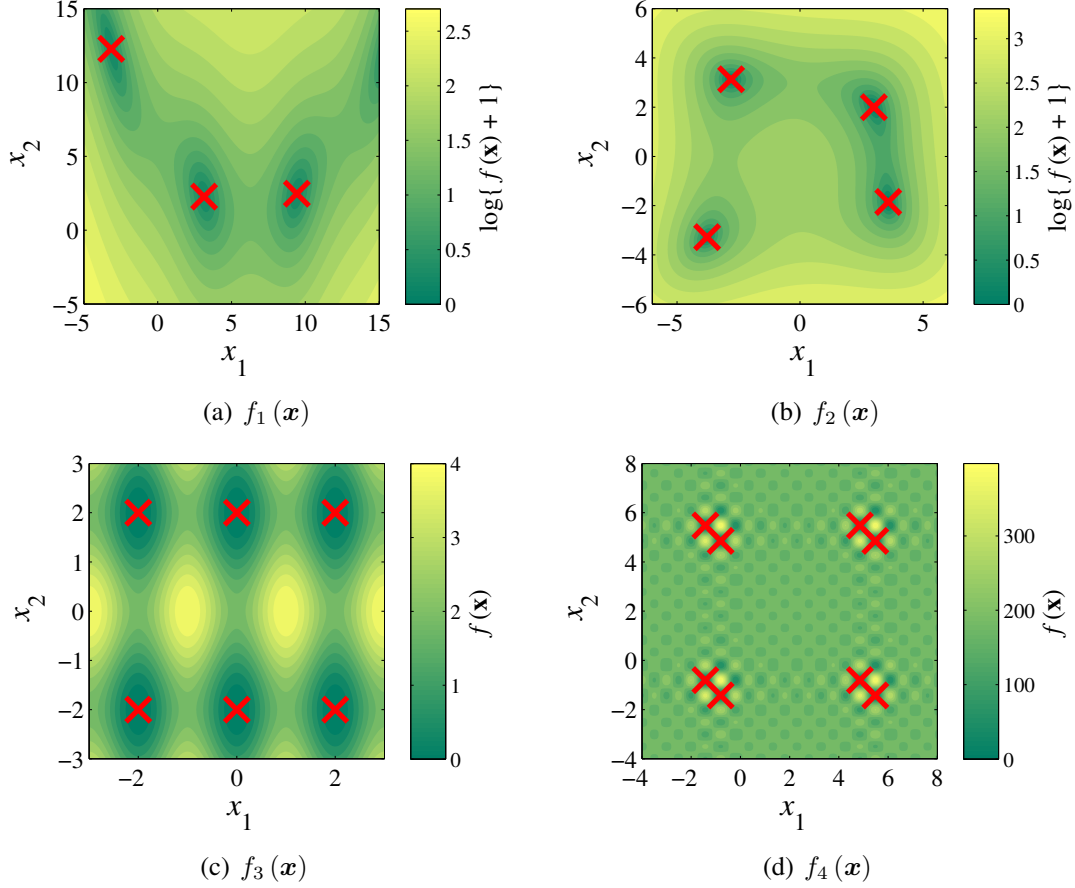


Fig 3.4: Contour maps of the benchmark functions where the red crosses denote the multi-solution.

3.5.2 Results

We have carried out trials by changing the P_{sw} in the benchmark functions. The simulation results are summarized in Fig. 3.7. The experimental results indicate that the long switching distance leads to improved #SOL on all benchmarks. It indicates that the slow information transmission is effective.

3.6 Conclusions

In this paper, we have studied the PSO with switched topology and defined the switching distance which corresponds to the average distance of the normal graph. Generally, since switched topology has the time-variant disconnected edge, the average distance cannot be calculated. However we quantified the distance using a switching rate as "switching distance". We applied the switched topology to the MSP and clarified the relation between the switching distance and its searching performance. The simulation results indicate that the longer switching distance leads to the improved performance. In the same switching distance, the results are different in each topology. It represents that only the switching distance cannot evaluate the topology. It needs further consideration.

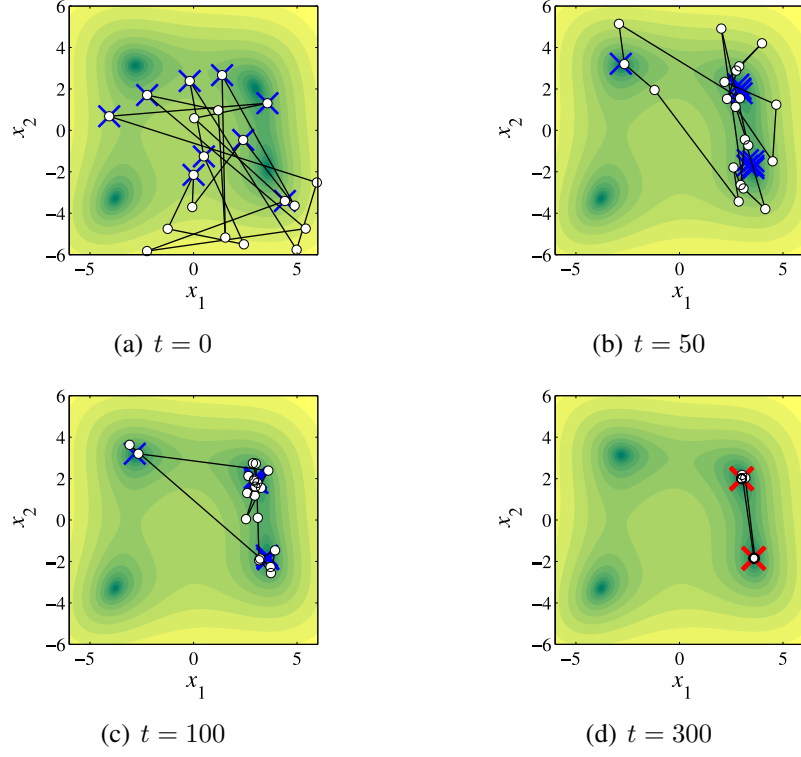


Fig. 3.5: Search process of $f_2(\mathbf{x})$ using the normal ring topology ($P_{\text{sw}} = 100\%$). Blue crosses denote L_{best} . Solid lines denote branch of switch-on. Dotted lines denote branch of switch-off. Red crosses denote solutions are found.

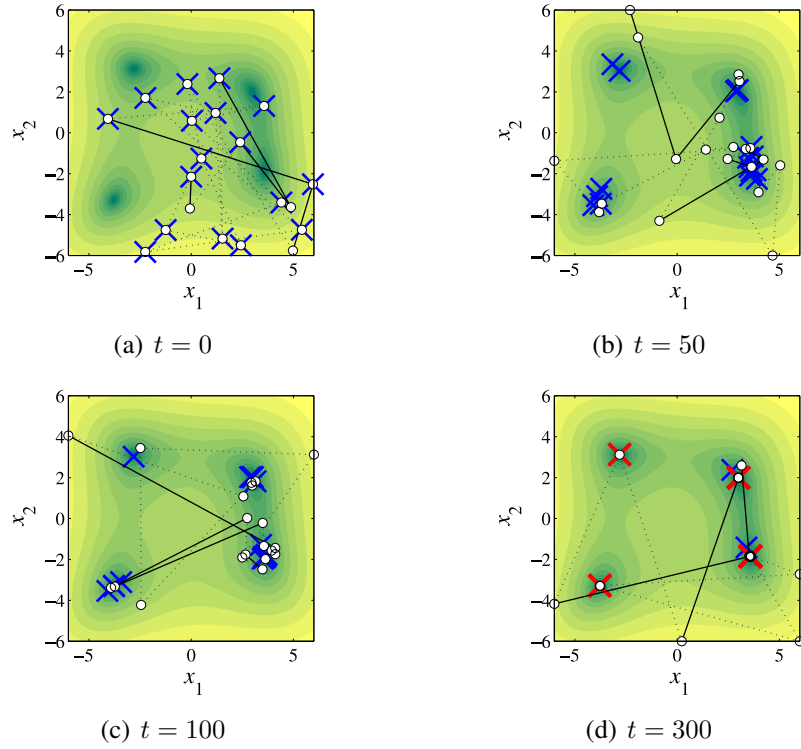
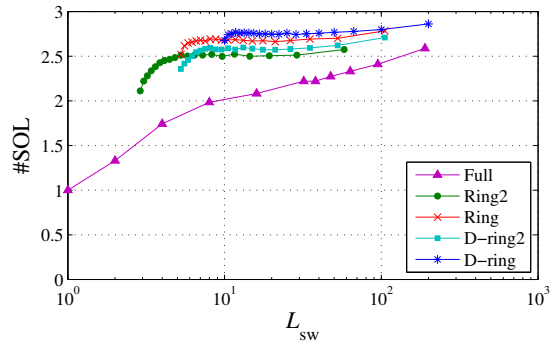
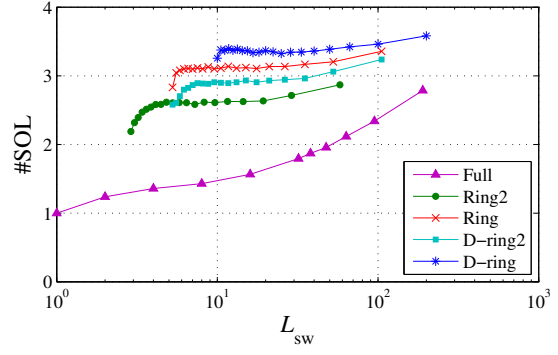


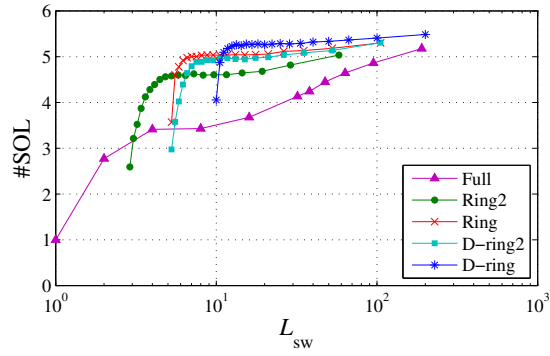
Fig. 3.6: Same as Fig. 3.5 except for the switched ring topology ($P_{\text{sw}} = 25\%$).



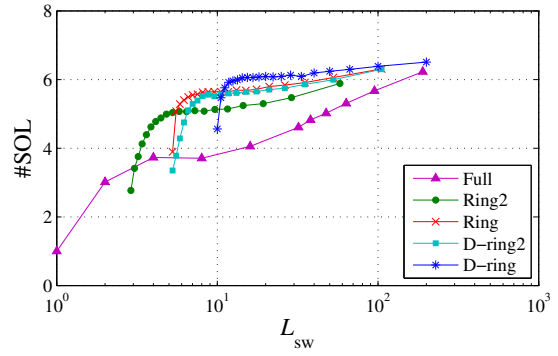
(a) $f_1(x)$



(b) $f_2(x)$



(c) $f_3(x)$



(d) $f_4(x)$

Fig. 3.7: The average distance effects the performance which is evaluated by the average number of the found optimal solutions (#SOL) for each benchmark functions. Full, Ring2, Ring, D-ring2 and D-ring are defined in Fig. 3.2.

参考文献

- [1] R. Sano, K. Jin'no and T. Saito, "Basic Characteristics of Deterministic PSO with Rotational Dynamics," in Proc. IEICE NOLTA, pp. 564-567, 2011.
- [2] R. Sano, T. Shindo, K. Jin'no and T. Saito, "PSO-based Multiple Optima Search Systems with Switched Topology," in Proc. IEEE CEC, pp. 3301-3307, 2012.
- [3] R. Sano, K. Jin'no and T. Saito, "Particle Swarm Optimization with Switched Topology and Deterministic Parameters," in Proc. IEEE SMC, pp. 530-535, 2012.
- [4] J. Kennedy and R. Eberhart, "Particle swarm optimization," in Proc. IEEE ICNN 1995, pp. 1942-1948, 1995.
- [5] J. Kennedy, "The particle swarm: Social adaptation of knowledge," in Proc. ICEC 1997, pp. 303-308, 1997.
- [6] A. P. Engelbrecht, "Fundamentals of Computational Swarm Intelligence," Willey, 2005.
- [7] H. Qin, J.W. Kimball and G.K. Venayagamoorthy, "Particle swarm optimization of high-frequency transformer," in Proc. 36th Annu. Conf. IEEE Ind. Electron. Soc., pp. 2908-2913, 2010.
- [8] M. Clerc, and J. Kennedy, "The Particle Swarm. Explosion, Stability, and Convergence in a Multidimensional Complex Space," IEEE Trans. Evol. Comput., vol. 6, no. 1, pp. 58-73, 2002.
- [9] K. Jin'no, "A novel deterministic particle swarm optimization system," Journal of Signal Processing, 13, 6, pp. 507-513, 2009.
- [10] K. Jin'no and T. Shindo "Analysis of dynamical characteristic of canonical deterministic PSO," in Proc. IEEE CEC, pp. 1105-1110, 2010.
- [11] T. Tsujimoto, T. Shindo, and K. Jin'no, "The Neighborhood of Canonical Deterministic PSO," in Proc. IEEE CEC, pp. 1811-1817, 2011.
- [12] V. Kadirkamanathan, K. Selvarajah, and P.J. Fleming, "Stability Analysis of the Particle Dynamics in Particle Swarm Optimizer," IEEE Trans. Evol. Comput., vol. 10, no. 3, pp. 245-255, 2006.
- [13] K.E. Parsopoulos and M.N. Vrahatis, "On the computation of all global minimizers through particle swarm optimization," IEEE Trans. Evol. Comput., vol. 8, no. 3, pp. 211-224, 2004.
- [14] D. Parrott and X. Li, "Locating and tracking multiple dynamic optima by a particle swarm model using speciation," IEEE Trans. Evol. Comput., vol. 10, no. 4, pp. 440-458, 2006.

- [15] X.D. Li, "Niching without niching parameters: particle swarm optimization using a ring topology," *IEEE Trans. Evol. Comput.*, vol. 14, no. 1, pp. 150-169, 2010.
- [16] S. Yang and C. Li, "A clustering particle swarm optimizer for locating and tracking multiple optima in dynamic environments," *IEEE Trans. Evol. Comput.*, vol. 14, no. 6, pp. 959-974, 2010.
- [17] M. Kubota and T. Saito, "A Discrete Particle Swarm Optimizer for Multi-Solution Problems," *IEICE Trans. Fundamentals*, E95-A, 1, pp. 406-409, 2012.
- [18] H. Matsushita and T. Saito, "Application of Particle Swarm Optimization to Parameter Search in Dynamical Systems," *NOLTA, IEICE*, E94-N, 10, pp. 458-471, 2011.
- [19] B.A. Garro, H. Sossa and R.A. Vazquez, "Design of artificial neural networks using a modified particle swarm optimization algorithm," in *Proc. IEEE-INNS Joint Conf. Neural Netw.*, pp. 938-945, 2009.
- [20] K. Ono, K. Jin'no and T. Saito, "Growing particle swarm optimizers for multi-objective problems in design of DC-AC inverters", *IEICE Trans. Fundamentals*, E94-A, 1, 2011.
- [21] D.J. Watts, S.H. Strogatz, "Collective dynamics of 'small-world' networks," *Nature* 393, pp. 440-442, 1998.
- [22] D. Beasley, D.R. Bully and R.R. Martinz, "A Sequential Niche Technique for Multimodal Function Optimization," *Evolutionary computation*, vol. 1, no. 2, pp. 101-125, 1993.
- [23] D. Cvijović and J. Klinowski, "Taboo Search: An Approach to the Multiple Minima Problem," *Science* vol. 267(5198), pp. 664-666, 1995.
- [24] J. Barhen, V. Protopopescu and D. Reister, "TRUST: A Deterministic Algorithm for Global Optimization," *Science* vol. 276(5315), pp. 1094-1097, 1997.

研究業績

(原著論文)

- T. Shindo, R. Sano, T. Saito and K. Jin'no, "Improvement in Solution Search Performance of Deterministic PSO using a Golden Angle," Journal of Signal Processing, Vol. 16, No. 4, pp. 299-302, July, 2012.

(国際会議)

- R. Sano, K. Jin'no and T. Saito, "Basic Characteristics of Deterministic PSO with Rotational Dynamics," in Proc. IEICE NOLTA, pp. 564-567, 2011.
- T. Shindo, R. Sano, T. Saito and K. Jin'no, "Improvement in Solution Search Performance of Deterministic PSO using a Golden Angle," in Proc. NCSP, pp. 473-476, 2012.
- R. Sano, T. Shindo, K. Jin'no and T. Saito, "PSO-based Multiple Optima Search Systems with Switched Topology," in Proc. IEEE CEC, pp. 3301-3307, 2012.
- K. Maruyama, R. Sano and T. Saito, "Deterministic Discrete Particle Swarm Optimizers with Collision and Insensitivity," in Proc. NDES, pp. 245-248, 2012.
- R. Sano, K. Jin'no and T. Saito, "Particle Swarm Optimization with Switched Topology and Deterministic Parameters," in Proc. IEEE SMC, pp. 530-535, 2012.

(国内発表)

- 佐野 亮介, 神野 健哉, 斎藤 利通, "正準形決定論的 PSO の回転数パラメータの効果について," 電子情報通信学会 非線形問題研究会 (NLP), 鳥取, 2010. 12.
- 佐野 亮介, 神野 健哉, 斎藤 利通, "回転動作を用いた確定論的 PSO," 電子情報通信学会 総合大会, 東京, 2011. 3.
- 丸山 一紀, 佐野 亮介, 斎藤 利通, "鈍感な粒子群最適化について," 電子情報通信学会 ソサイエティ大会, 北海道, 2011. 9.
- 進藤 卓也, 佐野 亮介, 斎藤 利通, 神野 健哉, "正準形決定論的 PSO の解探索能力," 電子情報通信学会 ソサイエティ大会, 北海道, 2011. 9.
- R. Sano, K. Jin'no and T. Saito, "Deterministic PSO-based Multiple Optima Search with Elite Preservation Strategy," Proc. of IEEE Workshop on Nonlinear Circuit Networks (NCN'11), pp. 40-43, 2011. 12.

- 丸山 一紀, 佐野 亮介, 斎藤 利通, ”鈍感な粒子群最適化と複数解問題,” 電子情報通信学会 非線形問題研究会 (NLP), 福島, 2012. 1.
- 神野 健哉, 辻本 貴博, 進藤 卓也, 佐野 亮介, 斎藤 利通, ”PSO のネットワーク構造と探索性能の関係に関する考察” 電子情報通信学会 非線形問題研究会 (NLP), 長崎, 2012. 3.
- 丸山 一紀, 佐野 亮介, 斎藤 利通, ”鈍感な決定論的離散粒子群最適化法,” 回路とシステムワークショップ論文集, pp. 267-269, 兵庫, 2012. 7.
- 佐野 亮介, 神野 健哉, 斎藤 利通, ”スイッチトトポロジーを導入した粒子群最適化法の複数解探索能力” 電子情報通信学会情報処理学会 情報科学技術フォーラム (FIT), 東京, 2012. 9.
- R. Sano, K. Jin'no and T. Saito, ”Particle Swarm Optimization based on Switching Connection,” Proc. of IEEE Workshop on Nonlinear Circuit Networks (NCN'12), pp. 51-54, 2012. 12.

謝辞

本論文は著者が法政大学大学院 工学研究科 電気工学専攻に在学中の2年間，同大学理工学部 電気電子工学科教授 斎藤利通博士の指導下で行ったものである．研究活動を遂行するにあたり，同教授から終始懇切に御指導，御鞭撻下さった同博士に深謝致します．

また，研究活動中に貴重な御助言・御討論を賜りました日本工業大学 工学部 電気電子工学科教授 神野健哉博士には深く感謝の意を表明いたします．

最後に法政大学 理工学部 電気電子工学科 斎藤利通研究室の皆様には様々に有益な御討論・ご助言を戴きました．ここに深謝致します．